Asian Journal of Aquatic Sciences, December 2024. Vol 7, Issue (3) 422-431
e-issn: 2716-4608
p-issn: 2655-366X

INTERANNUAL VARIABILITY OF SEA LEVEL ANOMALY (SLA) IN THE WESTERN SUMATRA COASTAL WATERS DRIVEN BY ENSO AND IOD MODULATIONS

Nabila Afifah Azuga[1*], Ahmad Dhuha Habibullah[2]
[1]Department of Marine Sciences, Faculty of Fisheries and Marine,
Universitas Riau, Pekanbaru, 28293 Indonesia
[2]Earth Science Study Program, Faculty of Earth Sciences and Technology,
Institut Teknologi Bandung, Bandung, 40132 Indonesia
*nabila.afifahazuga@lectrurer.unri.ac.id

ABSTRACT

This study aims to investigate the interannual variability of Sea Level Anomaly (SLA) along the western coast of Sumatra waters, focusing on the influences of the El Niño-Southern Oscillation (ENSO) and the Indian Ocean Dipole (IOD) in modulating SLA patterns. Using 31 years (1993-2023) of a gridded dataset from Copernicus Marine Service (CMS) and climate indices as the reference, the interplay between SLA and climate modes (ENSO and IOD) was determined through lag/lead correlation and spatial distribution analysis. The analysis shows a clear inversive relationship between ENSO and SLA, with a one-month delayed negative correlation (r= -0.41), indicating that SLA increases during the La Niña phase due to shifting in atmospheric and oceanic conditions. Similarly, SLA exhibits a negative correlation with DMI (r= -0.46) without any lag, suggesting a rapid response of SLA to IOD. Spatial analysis further demonstrates that ENSO and IOD most strongly influence SLA along Sumatra's coast within the first 1–3 months. These findings reveal that ENSO and IOD modulate SLA variability with distinct spatiotemporal characteristics, providing crucial insights for understanding coastal dynamics and enhancing mitigation strategy for sea level-related disasters in the western coastal region of Sumatra.

Keywords: Sea Level Anomaly, IOD, ENSO, Sumatra Region

1. INTRODUCTION

The waters off the western coast of Sumatra exhibit substantial interannual variability in sea level anomaly (SLA), which is more likely driven by the complex interactions between significant climate modes, such as the Indian Ocean Dipole (IOD) and El Niño-Southern Oscillation (ENSO)[1]. SLA represents the deviation of sea surface height (SSH) from the mean sea surface height (MSSH), measured relative to an ellipsoid as the mathematical reference surface. The variability of SLA is influenced by the unique geographical characteristics of each region, making it a critical factor in understanding ocean dynamics[2-3].

The interannual variability of SLA in coastal regions is a precarious aspect of oceanographic research, particularly in climate change and its associated phenomena. The western coast of Sumatra waters serves as a significant case study due to their susceptibility to climatic oscillations such as ENSO and the IOD. These oscillations are known to influence sea surface temperatures (SST) and, consequently, SLA through mechanisms that involve a complex interplay between atmospheric and oceanic processes[4]. ENSO is characterized by periodic fluctuations in SST across the central and eastern Pacific Ocean, which profoundly alters global weather patterns and ocean dynamics[5].

Received : 2 November 2024
Accepted : 5 December 2024

This also includes the changes in the Indonesian Through Flow (ITF) transport due to the difference in sea level between the eastern part of the Indian Ocean and the western part of the Pacific Ocean[6]. The variability associated with ENSO can lead to significant changes in SLA, particularly during extreme events such as El Niño and La Niña. For instance, during the 1997-1998 El Niño, pronounced SLA anomalies were observed, highlighting the direct influence of these climatic events on regional sea levels [5,7]. Similarly, IOD, which is defined by the temperature differences between the western and eastern Indian Ocean, also influences SLA changes in the surrounding coastal areas, including western Sumatra[8].

Much research has demonstrated that the interaction between ENSO and IOD can lead to compounded effects on SLA, with each phenomenon influencing the intensity and duration of the other. For example, the interannual variability of SST in the Indian Ocean can enhance the development of El Niño events, thereby exacerbating SLA fluctuations in adjacent coastal regions[4,8]. Each phase of ENSO and IOD has a different impact on the SLA. For example, when El Niño (IOD positive) occurs, the level of the sea surface decreases. Meanwhile, when La Niña (IOD negative) occurs, the level of sea surface increases[9,10].

According to Liu et al.[11]; Azuga & Radjawane[12]; Habibullah et al.[13], the dynamics of heat anomaly propagation due to ENSO and IOD indicate diverse temporal characteristics, particularly in their influence on the western coast of Sumatra waters. During the El Niño phase of ENSO, heat anomalies generated in the equatorial Pacific follow a complex path before reaching the southern part of the Indonesian region, including the western coast of Sumatra waters. These anomalies face interactions with oceanic and atmospheric processes that delay their arrival by approximately 7 to 9 months. This lag is likely caused by the slower east-to-west propagation of anomalies through ocean currents and teleconnection processes. In contrast, the IOD phenomenon, which originates in the Indian Ocean, exhibits a much more direct influence on the same region, including the western coast of the Sumatra region. The heat anomalies from IOD events propagate swiftly to the western coast of Sumatra waters without any lag time, recorded as a lag time of 0 months. This immediate impact reflects the IOD phenomenon's localized nature compared to the broader geographic scope of ENSO.

However, the effects of ENSO and IOD on SLA in this region remain insufficiently explored. Therefore, this research aims to analyze the interannual variability of SLA and their relation to ENSO and IOD phenomena by examining the lag and lead times of these climatic anomaly events over 31 years (1993–2023).

2. RESEARCH METHOD

Location of Research

The study focuses on the waters off the western coast of Sumatra, a region spanning geographically from 92°E to 106°E and 7.5°S to 10°N. As illustrated in Figure 1, this area represents a significant portion of the eastern Indian Ocean. This is a key region for understanding the influence of ENSO and IOD phenomena on SLA.

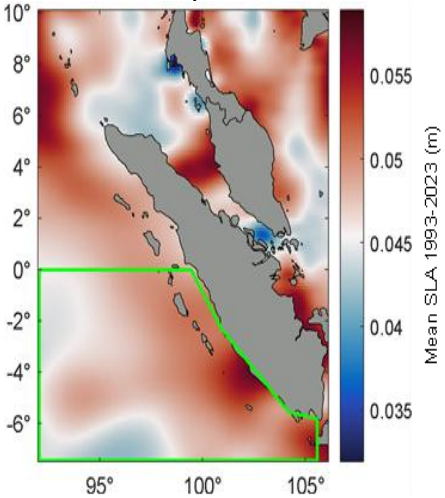

Figure 1. Research area: blue and green shades show SLA mean over the study period. The green polygon is the area of interest to be averaged and correlated with the climate indices.

This region is particularly dynamic due to its proximity to major climatic and oceanographic systems. It makes the area highly sensitive to changes driven by ENSO and IOD phenomena. The interplay of these systems influences not only sea level anomalies but also broader regional oceanographic and atmospheric conditions.

Procedures

Data Preparation

This research used a gridded dataset of Sea Level Anomaly (SST), derived from Copernicus Marine Service (CMS) Global Ocean Gridded L 4 Sea Surface Height and Derived Variables Reprocessed from 1993 to 2023 with a spatial resolution of 0.125˚ × 0.125˚ and can be retrieved from https://data.marine.copernicus.eu/product/SEALEVEL_GLO_PHY_L4_MY_008_047/services (accessed on November 27, 2024). The SLA data underwent preprocessing to ensure that it could be used in later calculations. This included temporal regrinding to align the datasets and eliminate gaps.

Niño 3.4 indices and Dipole Mode Indeks (DMI) were received from the National Oceanic and Atmospheric Administration (NOAA), available on (https://psl.noaa.gov/data/correlation/nina34.anom.data) and DMI, available on (https://psl.noaa.gov/gcos_wgsp/Timeseries/Data/dmieast.had.long.data) (accessed on November 27, 2024).

Area-Averaging

In order to emphasize the regional signal, SLA values were averaged over the study region along the western coast of Sumatra waters. We chose the area inside the green polygon in Figure 1 to be spatially averaged, ensuring consistency across the analyses. This spatial averaging helped to reduce noise and enhance the representation of broader regional anomalies while minimizing the influence of localized variability, such as those caused by mesoscale eddies or short-term wind events. By focusing on a well-defined area, this approach also allowed for a more robust comparison between the time series of SLA and the IOD index.

Lag/Lead Correlation Analysis

The relationship between SLA and both the Niño 3.4 index and DMI were analyzed using lag and lead correlation analysis, referred to Li et al.[14]; Azuga & Radjawane[12]; Habibullah et al.[13]. This step identified the time-lagged effects of ENSO and IOD phases on SLA. Cross-correlations were calculated for a range of time lags (positive and negative) to find out the potential lead or lag responses of the SLA to these climatic drivers. This analysis is conducted because of the teleconnection between the Pacific and Indian Oceans, where climatic anomalies originating in the Pacific require a lag time to propagate and influence conditions in the Indian Ocean.

To quantify the relationship between SLA and climatic indices (Niño 3.4 and DMI) over time, a cross-correlation function (XCF) was utilized[15]. The XCF measures the similarity between two-time series as a function of lag k, allowing us to analyze the delayed or advanced effects of ENSO and IOD on SLA. The lag k cross-covariance is estimated as:

$$c_{y_1y_2}(k) = \begin{cases} \frac{1}{T-k}\sum_{t=1}^{T-k}(y_{1,t}-\bar{y}_1)(y_{2,t+k}-\bar{y}_2), & k \geq 0 \\ \frac{1}{T+k}\sum_{t=1}^{T+k}(y_{2,t}-\bar{y}_2)(y_{1,t-k}-\bar{y}_1), & k < 0 \end{cases}$$

where $\bar{y}_1$ and $\bar{y}_2$ are the sample means of the series y_1 and y_2, respectively. To standardize the cross-covariance, the cross-correlation is computed as:

$$r_{y_1y_2}(k) = \frac{c_{y_1y_2}(k)}{s_{y_1}s_{y_2}},$$

where s_{y_1} and s_{y_2} are the sample standard deviations of y_1 and y_2.

Spatial Distribution of SLA

The spatial correlation analysis of SLA is aimed at analyzing the geographical variability of ENSO and IOD influences across the study region. Unlike a single averaged value, this approach reveals how different areas respond uniquely to ENSO and IOD. This will provide insights into

localized impacts and propagation patterns. By mapping SLA correlations, we can better understand the spatial modulation of these phenomena, particularly during El Niño/La Niña and positive/negative IOD phases, and identify regions most affected by these climatic events.

3. RESULT AND DISCUSSION

Lag and Lead Correlation between SLA and Nino 3.4

The relationship between SLA near the coast of Sumatra and Niño 3.4 index, as depicted in Figure 2, demonstrates a significant interannual variability influenced by ENSO. The first plot illustrates the time series of the Niño 3.4 index and SLA. The plot shows that there is an inverse relationship between Niño 3.4 and SLA, where positive periods of Niño 3.4 (El Niño events) conform to the decreases in SLA, while negative Niño 3.4 values (La Niña events) align with SLA increases. This suggests that ENSO significantly impacts SLA in the eastern Indian Ocean, including the western coast of Sumatra waters, likely through atmospheric and oceanic teleconnections.

The second plot, which shows the results of the cross-correlation analysis, provides further explanation of the relationship between SLA and ENSO phenomena. The coefficients of cross-correlation reveal a statistically significant negative correlation (r = -0.41); a strong relationship is observed when the SLA follows the ENSO by one month. This lag indicates a delayed oceanic response to ENSO-induced atmospheric anomalies. For instance, during an El Niño event, weakened trade winds and a shift in Walker Circulation dynamics[16,17], may cause a reduction in the thermocline depth and sea level near the Sumatra coast. However, this response takes time to propagate through the ocean, explaining the observed lag.

The delayed response of SLA also underscores the importance of understanding ocean-atmosphere dynamics in predicting regional sea level changes. The one-month lag may serve as a critical window for forecasting and mitigating the potential impacts of ENSO on coastal communities and marine ecosystems. For instance, lower-than-average SLA during El Niño events could expose coral reefs to increased thermal stress due to reduced water depths, while positive SLA during La Niña might enhance coastal flooding risks[18].

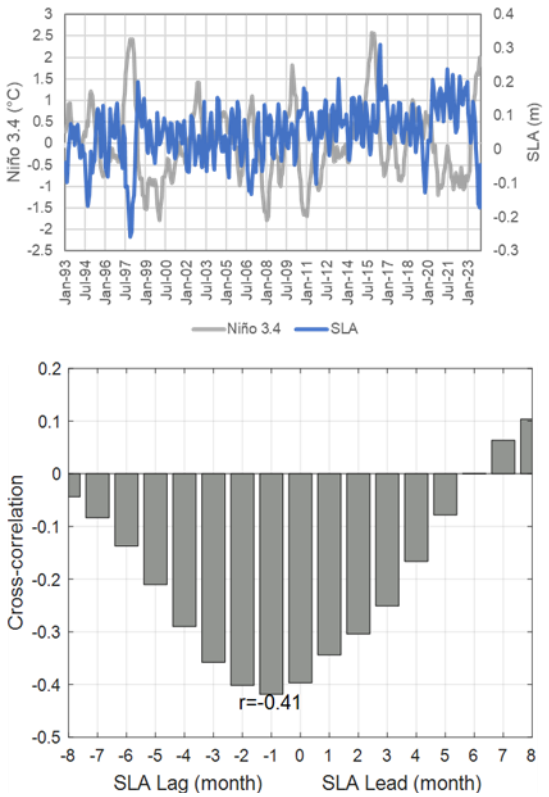

Figure 2. Lag/lead correlation between SLA and ENSO: blue and green shades show SLA mean over the study period. The green polygon is the area of interest to be averaged and correlated with the climate indices.

Numerous studies have confirmed that ENSO phenomena are linked to the shifting of Indian Ocean dynamics. For example, Ariska et al.[19] highlights the impact of ENSO's influence on rainfall patterns over Sumatra, indicating ENSO's role in altering atmospheric and oceanic interactions. Additionally, Kersale et al.[20] show ENSO's interplay with IOD, amplifying its effects on SST and rainfall

variability, which is directly related to SLA through atmospheric forcing and ocean circulation adjustments.

The correlation between SLA and ENSO also has broader implications for climate predictions. For example, improved monitoring of ENSO indices could help forecast coastal impacts such as flooding or erosion in Sumatra. It aligns with findings by Kersale et al.[20] that highlight the compounded effects of ENSO and IOD on Indonesian precipitation, which could affect the sea level. These predictive insights are vital given the region's socio-economic reliance on stable coastal and oceanic systems.

Lag and Lead Correlation between SLA and DMI

Figure 3 shows the linkage between SLA and the IOD, which the DMI and the SLA represent, on average, near the Sumatra coast in the eastern Indian Ocean. The time series plot shows fluctuations of DMI and SLA over 31 years (1993 to 2023), while the cross-correlation plot shows the evolution of the lead/lag relationship between DMI and SLA over 8 8-month windows. The strongest correlation between the IOD and SLA was observed at a 0-month lag.

The negative correlation (r = -0.46 at lag 0 months) suggests that during positive IOD events (characterized by cooler sea surface temperatures near Sumatra), SLA decreases near the Sumatra coast. This shows a strong response of coastal sea levels to the atmospheric and oceanic anomalies associated with the IOD, which is consistent with past studies. Previous work[21] how positive IOD events might induce upwelling and thermocline shoaling along the eastern Indian Ocean coast, leading to lower SLA. Conversely, during negative IOD phases, warm water accumulation elevates SLA in the region.

The significant negative lagged correlations up to -3 months further imply that SLA variability responds to IOD events within a short temporal window. This aligns with the past findings that identified the IOD's critical role in regulating regional thermocline depth and ocean circulation patterns in the Indian Ocean[22]. Additionally, the lack of significant positive correlations indicates that changes in SLA are largely influenced by direct interactions with IOD dynamics instead of feedback processes that involve delayed atmospheric factors.

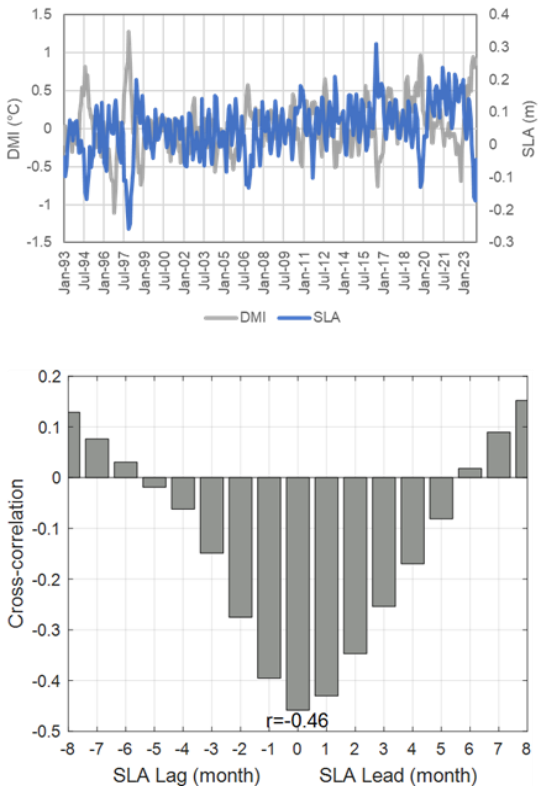

Figure 3. Lag/lead correlation between SLA and IOD: blue and green shades show SLA mean over the study period. The green polygon is the area of interest to be averaged and correlated with the climate indices.

Spatial Distribution of SLA in Relation to ENSO

Figure 4 shows the spatial correlation between ENSO and SLA Sumatra across different lag intervals, ranging from no lag to an 8-month lag. Each panel shows the distribution of correlation coefficients, with a colour bar indicating the strength and direction of the correlations (red/blue represents positive/negative correlation).

The black dots indicate statistically significant correlations ($p < 0.01$).

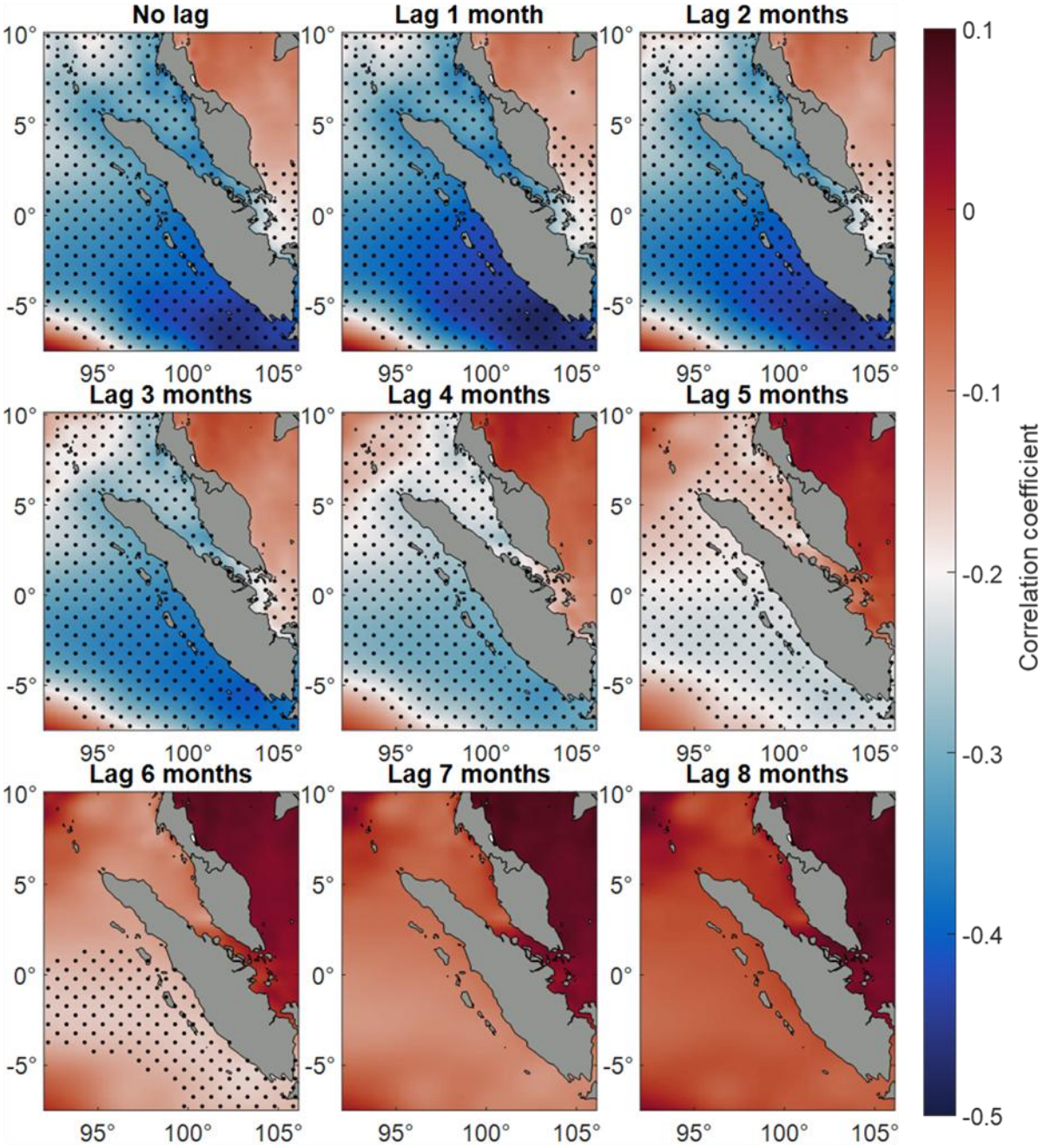

Figure 4. Spatial correlation maps between SLA and Niño 3.4 at various lags (0 to 8 months), with dotted areas indicating significant correlations and a colour scale representing the correlation coefficient

The Figure shows how the Niño 3.4 index, representing ENSO, influences Sea Level Anomaly (SLA) along the western coast of Sumatra over 0 to 8 months. The strongest negative correlations are shown in dark blue. During the first two months, the strongest negative correlation is observed near the coast. This indicates a significant decrease in SLA in response to ENSO, with the effects being strongest and most localized during this early period.

From 3 to 5 months, the negative correlation weakens but spreads farther offshore. Beyond the 3-month lag, the

correlations begin to weaken significantly. By the 4-month lag, the spatial coherence of the negative correlation diminishes, and by the 5-month lag, most of the region exhibits low or near-zero correlations.

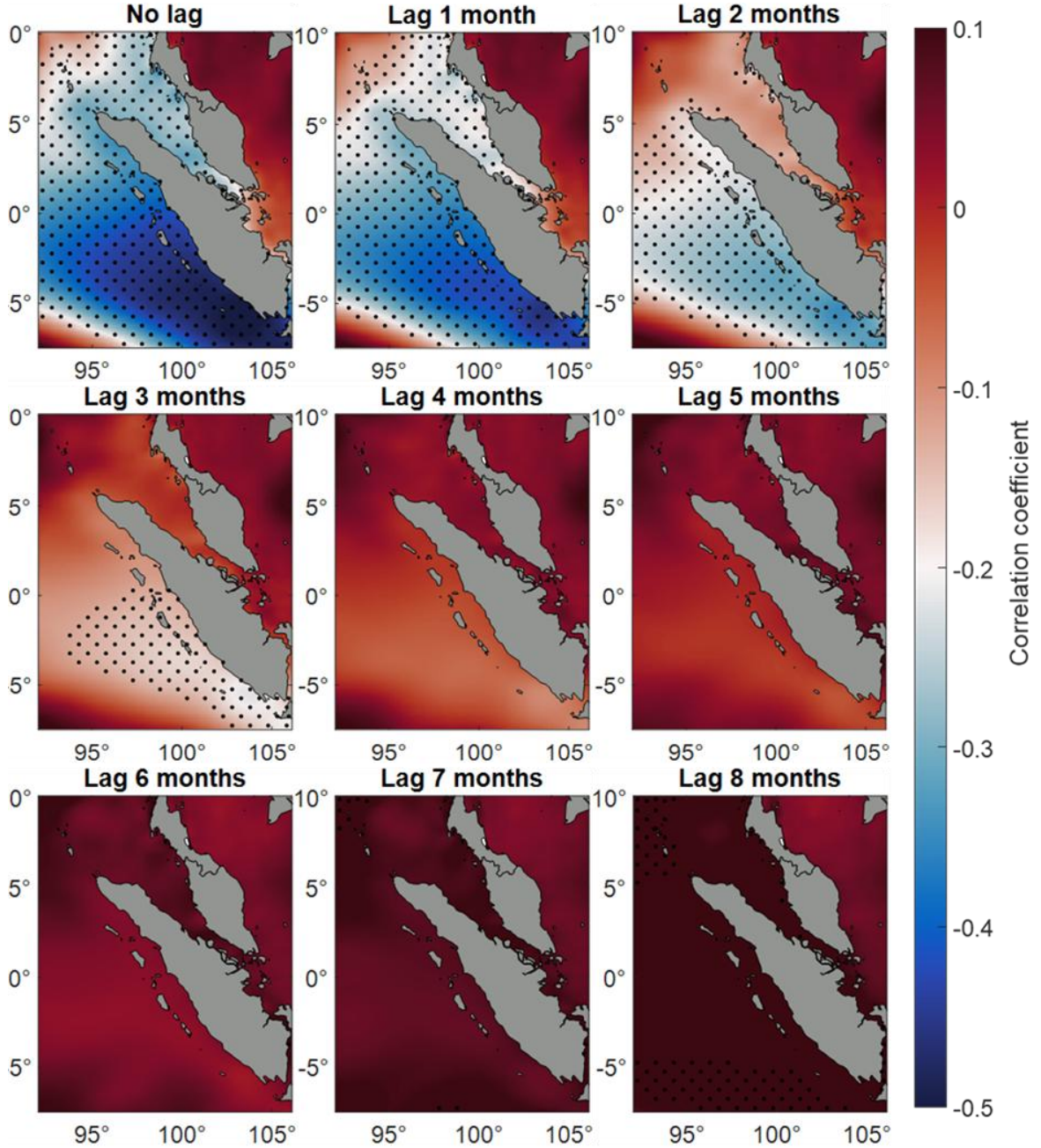

Figure 5. Spatial correlation maps between SLA and DMI at various lags (0 to 8 months), with dotted areas indicating significant correlations and a colour scale representing the correlation coefficient.

From the 6-month lag onward, the spatial distribution of correlations becomes predominantly insignificant, with no strong patterns observed. This indicates that the influence of ENSO on SLA dissipates after approximately three months, consistent with a temporal limit on the teleconnection's strength and significance.

This spatial analysis explains the temporal and spatial specificity of ENSO's influence on SLA near Sumatra, peaking around 1–3 months and declining rapidly subsequently. The presence of statistically

significant correlations ($p<0.01$) within the first few months proves the robustness of this relationship during the short lag window. This finding aligns with Nurlatifah et al.[23], which found the observed pattern along the southern waters of Java, which shares oceanographic characteristics with the Sumatra region.

The research found that during the El Niño events, there was a significant decrease in sea level, with the most pronounced effects observed within a 0 to 2-month lag. A similar pattern was also found in Barskar et al.[24], which demonstrated that the principal component (PC) corresponding to the first mode leads the second mode by approximately five months, indicating a temporal relationship influenced by ENSO phenomena.

Spatial Distribution of SLA in Relation to IOD

Figure 5 shows the spatial distribution of the correlation between the DMI and SLA in the eastern Indian Ocean for a lag time ranging from 0 to 5 months. The colour scale represents the correlation coefficients, with blue indicating strong negative correlations (down to -0.5) and red indicating weak positive correlations (up to 0.1). Black dots highlight areas where the correlation is statistically significant, with p-values less than 0.01. At lag 0 months (no lag), a strong negative correlation is observed along the coast of Sumatra and surrounding areas, indicating an immediate and robust response of SLA to IOD variability.

The significant correlation regions, marked with black dots, are widespread along the eastern Indian Ocean, particularly near the Sumatra coastline. This is in line with the previous research conducted by Duan et al.[25], which found that the IOD induces significant sea level changes in the waters around the Indian Ocean, with positive IOD events leading to sea level rise in the western side of the Indian Ocean and corresponding to the decreasing in sea level in the eastern of Indian Ocean.

At lag 1 month, the negative correlation persists but slightly weakens in intensity, with the significant region still concentrated along the coastal zones. By lag 2 months, the negative correlation becomes weaker, and the extent of statistically significant regions decreases. This reflects a gradual decline in the influence of IOD on SLA. By lag 3 months, the correlations are minimal, and most regions lose statistical significance. It means that the relationship between IOD and SLA dissipates substantially after three months.

At lags 4 and 5 months, the correlations become negligible, with no significant areas remaining. At this time window, the SLA near Sumatra is no longer directly influenced by IOD variability. This pattern highlights the short-term nature of the coupling between IOD and SLA in this region, with the strongest and most significant effects occurring within the first three months following IOD events.

4. CONCLUSION

This study reveals a consistent negative correlation, with SLA lagging Niño 3.4 by approximately 1-2 months. Meanwhile, SLA shows a negative correlation with DMI without any lag. The spatial analysis illustrates the influence of Niño 3.4 and DMI on SLA with distinct spatial variations in correlation strength and significance, which explain the potential of these climate anomaly phenomena as a predictive tool for regional SLA variations.

However, this study acknowledges limitations, including the reliance on linear correlations and the exclusion of other climate drivers that may influence SLA. Future research should explore the integration of additional climatic indices, non-linear methodologies, and longer time series to enhance understanding and predictive accuracy. Overall, this work contributes to advancing our knowledge of climate-ocean interactions and supports informed decision-making for climate-resilient planning in vulnerable coastal areas.

REFERENCES

1. Wisha, U.J., Wijaya, Y.J., & Hisaki, Y. Sea Level Variability in the Equatorial Malacca Strait: The Influence of Climatic–Oceanographic Factors and Its Implications for Tidal Properties in the Estuarine Zone. *Climate*, 2023; *11*(3): 3-21.
2. Church, J.A., & White, N.J. Sea Level Rise from The Late 19th to the Early 21st Century, *Surv. Geophys*, 2011; *32*: 585–602.
3. Sarsito, D.A., Prijatna, K., Wijaya, D.D., Fajar, N., Radjawane, I.M., & Windupranata, W. Long Term Variation of Sea Level Anomaly (September 1992- January 2017) in the Indonesian Sea from Multi-Mission Satellite Altimetry Data. *IOP Conference Series: Earth and Environmental Science*, 2018: 162: 012043.
4. Hong, X., Hu, H., Yang, X., Zhang, Y., Liu, G., & Liu, W. Influences of Indian Ocean Interannual Variability on Different Stages of El Niño: A Foam1.5 Model Approach. *Science China Earth Sciences*, 2014; 57(11): 2616-2627.
5. Triana, K. (2023). The Dynamic of Sea Level Anomaly in the Papua Coastal Area and Its Associated Response to The Climate Indices. *IOP Conference Series: Earth and Environmental Science*, 2023; *1251*(1): 012004.
6. Susanto, R.D., & Song, Y.T. Indonesian Throughflow Proxy from Satellite Altimeters and Gravimeters. *Journal of Geophysical Research: Oceans*, 2015; 120(4): 2844-2855.
7. Piecuch, C.G., & Ponte, R.M. Buoyancy-driven Interannual Sea Level Changes in the Southeast Tropical Pacific. *Geophysical Research Letters*, 2012; *39*(5): 1-5.
8. Murukesh, N., & Yuan, X. The Influence of the Indian Ocean Dipole on Antarctic Sea Ice. *Journal of Climate*, 2015; 28(7): 2682-2690.
9. Fadlan, A., Sugianto, D.N., & Zainuri, M. Influence of ENSO and IOD to Variability of Sea Surface Height in the North and South of Java Island. *IOP Conference Series: Earth and Environmental Science*, 2017; 55(1): 012021.
10. Mujiasih, S., Ismail, M.F.A., Basit, A., Ratnawati, H.I., Hatmaja, R.B., & Lekalette, J. D. Long-Term Trend and Variability of Ocean Heat Content in the Indonesian Maritime Continent. *IOP Conference Series: Earth and Environmental Science*, 2023; 1245(1), p. 012043).
11. Liu, Q.Y., Feng, M., Wang, D., & Wijffels, S. Interannual Variability of the Indonesian Throughflow Transport: A Revisit Based on 30-year Expendable Bathythermograph Data. *J. Geophys. Res. Oceans*, 2015; 120: 8270–8282.
12. Azuga, N.A., & Radjawane, I.M. Subsurface Marine Heatwaves of South Java Sea: Trend, Frequency, Duration, and Cumulative Intensity Based on Assimilation Model (1993-2019). *Jurnal Perikanan dan Kelautan*, 2022; *27*(3): 394-406.
13. Habibullah, A.D., Tarya, A., Ningsih, N.S., & Putri, M.R. Marine Heatwaves in the Indonesian Fisheries Management Areas. *Journal of Marine Science and Engineering*, 2023; 11(1): 161.
14. Li, Y., Ji, R., Fratantoni, P.S., Chen, C., Hare, J.A., Davis, C.S., & Beardsley, R.C. Wind-Induced Interannual Variability of Sea Level Slope, Along-Shelf Flow, and Surface Salinity on the Northwest Atlantic Shelf. *Journal of Geophysical Research-Oceans*, 2014; 119(4): 2462-2479.
15. MathWorks. Cross-correlation function. *MathWorks Documentation*. Retrieved December 6, 2024,
16. Mock, C.J. The Role of the Walker Circulation in the El Niño-Southern Oscillation. *Journal of Climate*, 2007; 20(15): 3721-3736.
17. Lau, K.M., & Yang, S. *Walker Circulation*. *In Holton JR (ed) Encyclopedia of Atmospheric Sciences*. Academic Press, 2003; 2505-2510
18. Nicholls, R. J., & Cazenave, A. Sea-Level Rise and its Impact on Coastal Zones. *Science*, 2010; *329*(5992):628-628.

19. Ariska, M., Putriyani, F.S., Akhsan, H., Supari, S., Irfan, M., & Iskandar, I. Trend of Rainfall Pattern in Palembang for 20 Years and Link to El-niño Southern Oscillation (ENSO). *Jurnal Ilmiah Pendidikan Fisika Al-Biruni*, 2023; 12(1): 67-75.
20. Kersalé, M., Volkov, D.L., Pujiana, K., & Zhang, H. Interannual Variability of Sea Level in the Southern Indian Ocean: Local vs. Remote Forcing Mechanisms. *Ocean Science*, 2022; 18(1): 193-212.
21. McPhaden, M.J., Zebiak, S.E., & Glantz, M.H. ENSO as An Integrating Concept in Earth Science. *Science*, 2006; 314(5806): 1740-1745.
22. Saji, N.H., Goswami, B.N., Vinayachandran, P.N., & Yamagata, T. A dipole mode in the tropical Indian Ocean. *Nature*, 1999; 401(6751): 360-363.
23. Nurlatifah, A., Martono, M., Susanti, I., & Suhermat, M. Variability and Tren of Sea Level in Southern Waters of Java, Indonesia. *Journal of Southern Hemisphere Earth Systems Science*, 2021; 71(3): 272-283.
24. Barskar, H., Senapati, B., Kaundal, M., Amere, A.B., & Dash, M.K. Evolution of Tripole Pattern of Sea-Level Anomalies in the Indian Ocean During Concurrent ENSO-IOD Episodes. *Journal of the Indian Society of Remote Sensing*, 2023; 51: 383-394.
25. Duan, J., Li, Y., Zhang, L., & Wang, F. Impacts of the Indian Ocean Dipole on Sea Level and Gyre Circulation of the Western Tropical Pacific Ocean. *J. Climate*, 2020; 33: 4207-4228.